

The Construction and Application of a Pet Waste Collecting Drone Using STM32 for a Better Environment

Yiming Cai^{1,*}

¹Shanghai Starriver Bilingual School, Shanghai, China

*Corresponding author: alexfeialex@iCloud.com

Abstract: A drone recognizes and follows the pet using a camera under the drone and has add-on abilities to recognize and pick up the pet's feces or add a camera that connects over wifi. It uses an STM32 as the main control chip and an OpenMV camera to recognize shapes and colors. We used Apriltags to represent pets and their feces. In our test, 88% successfully followed the pet and recognized their waste, which shows that the system is fast and accurate.

Keywords: Drone, pet, clean community, Camera recognition, STM32

1. Introduction

The conventional method of attaching location trackers to a pet's neck has limitations due to size constraints and the inconvenience of replacing and charging them. To solve these challenges, the drone hovers above the pet during operation. This system offers full expandability and modularity such as an add-on camera for remote sensing.

While pet owners usually clean up for their pets, the drone system becomes especially helpful when owners are busy and unable to walk their dogs alone. In such scenarios, the drone picks up pet waste, contributing to a cleaner environment for the community.

By combining pet tracking and waste management in a single system, the drone-based solution not only simplifies the tasks for pet owners but also promotes responsible and considerate pet ownership within communities[1-2].

2. Function and Operation

After the drone unlocks and takes off, the OpenMV camera constantly looks for the pet and its feces. When there is no waste spotted yet, the drone will follow the pet and hover above it at an adequate height. When waste is spotted, the drone will collect the waste quickly. Then it continues to follow the pet.

For additional security, snapshots can be taken on the camera and stored on a MicroSD card for the owners to view. The overall operation of the drone is shown in Figure 1.

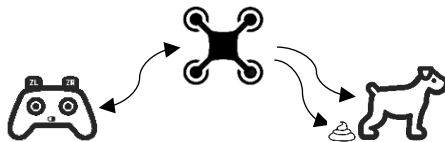


Figure 1: Overall operation of the drone

3. Hardware Design

The drone mainly comprises a lightweight UAV, an OpenMV camera module, an NRF2401 communication module, and a power module.

The UAV involves an STM32 main board, an MPU6050 gyroscope, and an optical sensor. STM32 stabilizes the drone using an advanced PID algorithm, using data from the gyroscope and optical sensor.

A click on the L key initiates the stabilization, where the optical sensor sends the relative velocity and the gyroscope sends the angle to STM32. STM32 calibrates the 4 rotor speeds using these statistics, allowing it to stay motionless when hovering.

OpenMV camera module recognizes and locates the pet and its waste. In this prototype, an Apriltag represents the pet and a red block represents the waste it leaves behind. The target location is sent to STM32 to navigate the drone. When OpenMV sends location data to STM32, it prioritizes the location of the waste, so that the drone picks up the waste when a pet leaves it behind and it will continue to follow the pet when the waste is cleared.

Then the location data from OpenMV is used to change the rotor speed to navigate it toward the target location.

The whole system is depicted in Figure 2 as shown below:

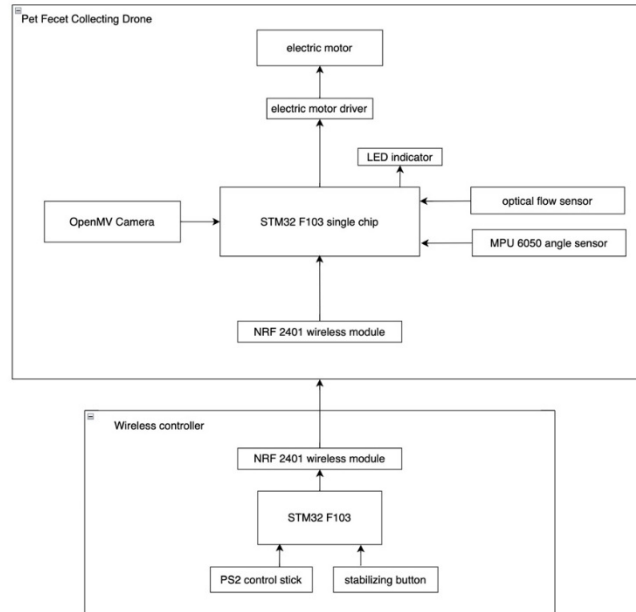


Figure 2: Interior electronic design map

3.1 Main Control MCU

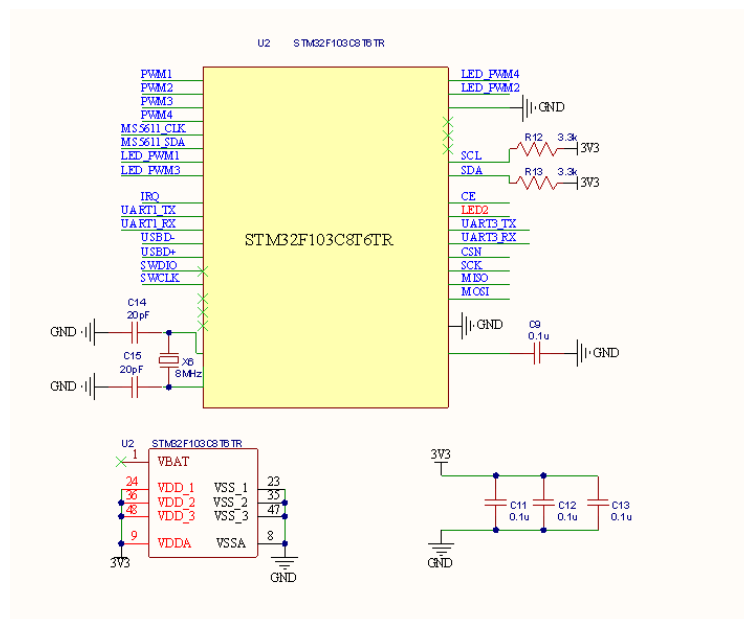


Figure 3: STM32C8T6 schematic diagram

STM32C8T6 used for the MCU is a high-performance Arm Cortex M4 32bit RISC microcontroller that operates at a staggering 84MHz frequency, where it balances both connectivity and functionality. ARM Cortex M4 features an FP computing unit, enabling it to calculate all sorts of precise data[3-4].

STM32C8T6 also comes with 256KB flash storage and 64KB SRAM, which provides plenty of room for complex applications. It features industry-standard I/O, including SPI and I2C connectors that drive the drone and peripherals. In conclusion, this STM32C8T6 is the perfect fit for our lightweight and powerful drone. The schematic diagram of STM32C8T6 is shown in the figure3.

The physical picture of the UAV flight control motherboard is shown in Figure 4

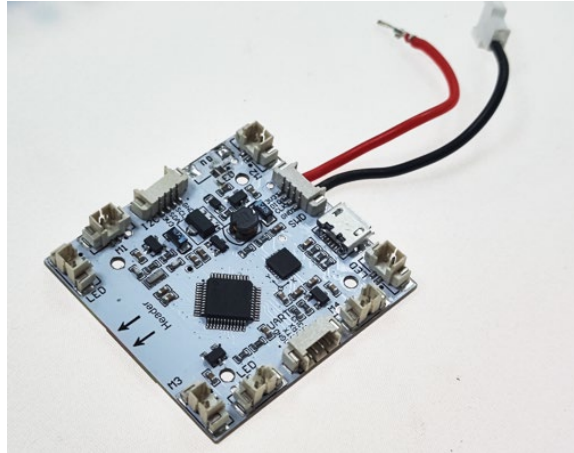


Figure 4: The physical picture of the UAV flight control motherboard

3.2 Drone Flight and Stabilization

The drone is equipped with a gyroscope MPU6050 and an optical flow sensor PWM3901.

MPU6050 is a nine-axis gyroscope that constantly gathers tilt, magnetism, acceleration, and air pressure. MPU6050 reads the 3-dimensional tilt and 3-dimensional acceleration data and sends it through a I2C connector to the STM32.

PWM3901 optical flow sensor provides the high-precision relative velocity of the drone.

By utilizing the data provided, the drone can calibrate the motor speeds that allow it to fly smoothly and hover steadily above the ground. The optical flow sensor is shown in Figure 5.

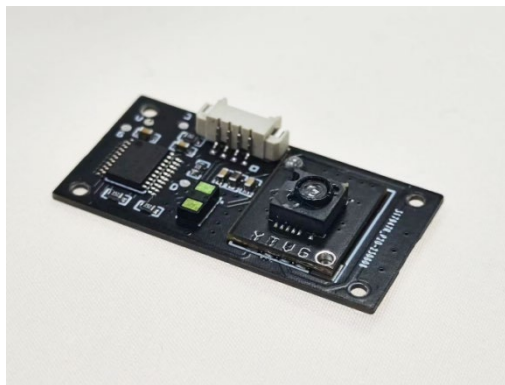


Figure 5: The optical flow sensor

3.3 Electric Motor

The drone is equipped with four 720 coreless brushed motors. To provide sufficient current to drive the motors, an NMOS transistor (SI2302) is selected to design the motor drive circuit. The circuit is controlled by generating PWM pulses through the STM32 F401CCU6 timer to control the opening and closing of the NMOS, thus achieving precise control of the brushed motors.

When the motor is in the off phase of the PWM, a small capacitor absorbs the generated energy

produced by the remaining kinetic energy of the motor. The motor control principle is shown in Figure 6.

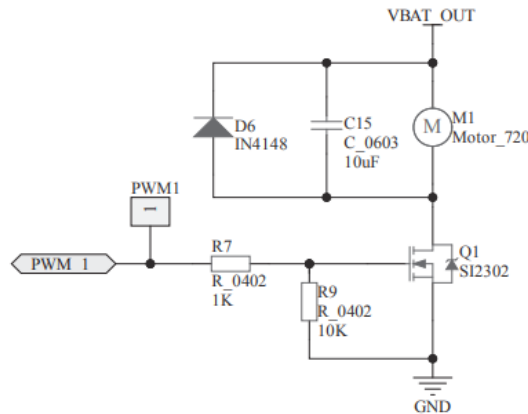


Figure 6: Motor control schematic diagram

3.4 Wireless Controller

RF24L01 is an ISM wireless chip operating at 2.4~2.5GHz. Its peak performance reaches up to 2 Mbps. The nRF24L01+ interface includes an IRQ pin, which indicates the signal of the nRF24L01+. When the IRQ pin is on a low level, it triggers an interruption. In the interrupt handling function, the program only sets the corresponding flag, and the actual processing of the interrupt is placed in the main code. When communicating with the STM32F103C8T6, it does not occupy the STM32 CPU, because adjustments such as frequency, transmission rate, and data package length are done directly on RF24L01. The schematic diagram of wireless communication is shown in Figure 7.

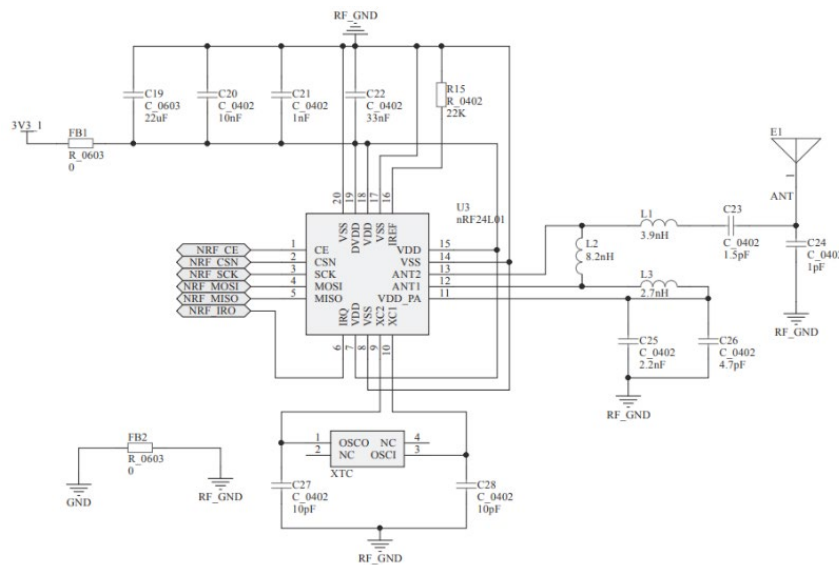


Figure 7: Schematic diagram of wireless communication

4. Software Design

At startup, the system calibrates the gyroscope and the MCU clock starts to operate. The wireless chip searches for signals from the controller. The 4 LED lights blink until an up-down swipe gesture on the left stick is done on the controller. This process unlocks the drone and the lights turn to a steady glow.

During the flight, the MCU STM32 combines data from the gyroscope and the optical sensor, where it goes through a float point PID calculation to produce PWM output values for each of the 4 motors. This operation repeats every 5 milliseconds to ensure a stable and smooth flight.

A click on the ZR key turns the pet tracking feature on. The camera looks for the apriltag or the red

block and reads its location and height. Then the drone uses this location and height to adjust its position to quickly fly above the target. The Pet Fecet Collecting Drone software design block diagram is shown in Figure 8.

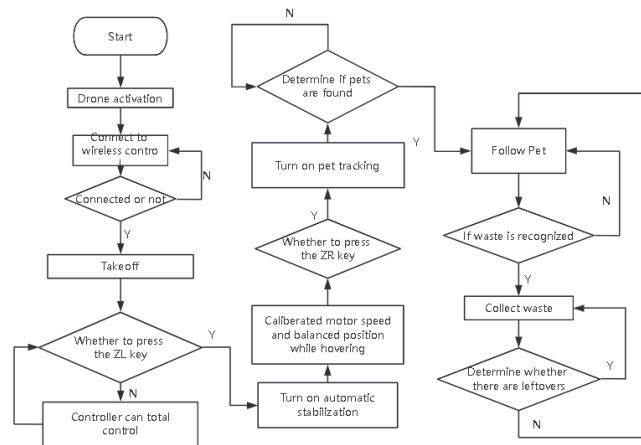


Figure 8: Pet Fecet Collecting Drone software design block diagram

4.1 Uav flight Attitude Calculation

Attitude calculation means that the MCU reads its sensor data and calculates the attitude Angle of the quadcopter in real-time, such as roll Angle, pitch Angle, and yaw Angle information. General attitude calculation can be divided into hardware solutions and software solutions. The hardware solution is to use the digital motion processor DMP of MPU6050, which can analyse the data from the gyroscope and accelerometer, and calculate the accurate quaternions based on the processing of the hardware circuit. The processing results can be read from the DMP memory. Although it is simple to use DMP to read the data, it cannot track the drastic attitude fluctuations of the aircraft. And sometimes there are drastic fluctuations and halts. Therefore, we will choose to use some software algorithms to solve the problem. Via the Kalman filter algorithm, the frequency response advantages of the accelerometer and gyroscope are individually utilized for each of the original data measured by the sensor, to improve the attitude accuracy of the data[5-6].

4.2 Quaternion Operation

Quaternion is a method of equivalent projection of attitude transformation through the multiplication of hypercomplex numbers. Compared with the Euler Angle description of attitude matrix, the latter requires a lot of trigonometric function calculation and there are singular points, so quaternion representation can reduce the complexity of attitude solution and achieve real-time flight attitude solution. The following is the quaternion rotation matrix:

$$\begin{bmatrix} q_w^2 + q_x^2 - q_y^2 - q_z^2 & 2(q_xq_y + q_wq_z) & 2(q_xq_z - q_wq_y) \\ 2(q_xq_y - q_wq_z) & q_w^2 + q_x^2 - q_y^2 - q_z^2 & 2(q_yq_z - q_wq_x) \\ 2(q_xq_z + q_wq_y) & 2(q_yq_z - q_wq_x) & q_w^2 - q_x^2 - q_y^2 + q_z^2 \end{bmatrix}$$

4.3 Servo System Control Design

The position and velocity parameters of the servo system are controlled by the classical proportional-integral-differential control method. The expected position is different from the measured position, and then the desired speed is output after proper adjustment by the position PID regulator. The expected speed is different from the present speed. After proper adjustment by the speed PID regulator, the corresponding pulse width modulation duty cycle and frequency value are output to the corresponding servo driver for motor drive control. Thus the servo system position control and speed control works together. The closed-loop control block diagram of the servo system position and speed is shown in Figure 9

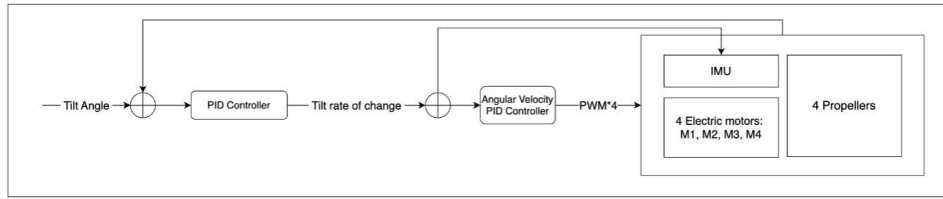


Figure 9: The closed-loop control block diagram of the servo system position and speed.

The input-output relationship of a classical PID controller is:

$$u(t) = K_p \cdot e(t) + K_i \int_0^t e(t) \cdot dt + K_D \cdot \frac{de(t)}{dt}$$

Where $u(t)$ is the output, K_p is the proportional coefficient, K_i is the integral coefficient, K_D is the differential coefficient, and $e(t)$ is the difference of the input quantity. In the control system, increasing K_p can speed up the response speed of the system, but too much K_p causes the system to overshoot, often needs to add K_i and K_D for adjustment, which can make the control system take into account the response speed at the same time can reduce the overshoot of the system, enhance the stability of the control system.

4.4 Pet recognition algorithm

In the pet recognition function, AprilTag is first attached to the pet through OpenMV to detect AprilTag and obtain the position of the pet in the image, to realize the positioning of the pet. At the same time, AprilTag's pose estimation function is used to obtain the pet's pose information relative to the camera, and the pet's motion tracking is realized by combining the image sequence. And use image processing and color filtering technology to realize the effect of pet feces recognition.

5. Experimental Testing and Analysis

The Apriltag is pasted on a remote-controlled car. Placed indoors in a closed environment, the car is programmed in a random direction with speeds below 1m/s, making frequent turns and stops to simulate real pet behavior. After about 2 minutes, a red square is dropped, and the car keeps traveling in the original pattern. This test simulates a real scenario that tests the drone's functionality. The camera recognition effect is shown in Figure 10.

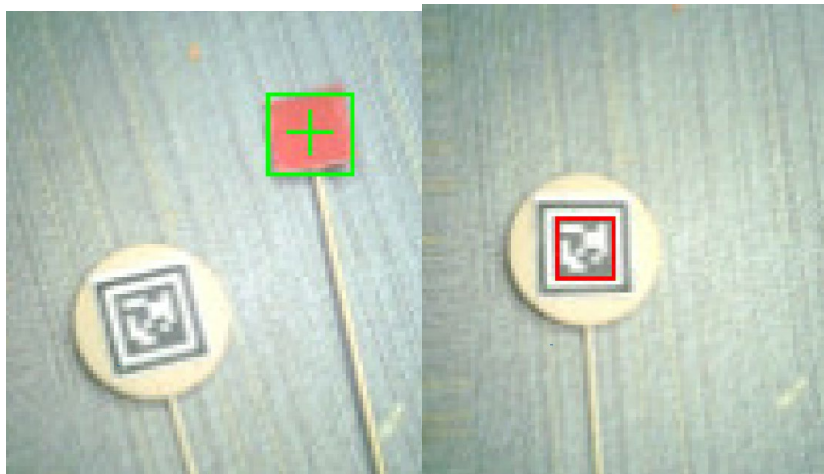


Figure 10: The camera recognition effect. The camera prioritizes the red square when both the red square and Apriltag are present.

5.1 Real World Test

In 90 tests made, 84 successfully followed close to the Apriltag, hovered above the waste, and turned on one of the LED lights to indicate that the drone successfully aligned with the waste and was ready to pick it up. The actual effect is shown in Figure 11.



Figure 11: The actual effect

The test results show that the system can accurately identify Apriltag for pet matching, and has a higher frame rate, which can meet the application scenarios of the system, and has a good recognition effect.

To test the real-time tracking effect of the system on pets. Pets wearing an Apriltag are tracked in an indoor environment, and the actual tracking effect of the drone is judged by counting the number of lost pets within two hours and the number of successfully recovered pets within three minutes after losing them. The test data are shown in Table 1.

Table 1: Track effect test data

Group	Number of tests	Average heel in two hours Pet loss times	Within three minutes of losing your pet Average number of recoveries
1	30	3.2	1.4
2	30	2.8	1.7
3	30	3.5	0.8

After the test, the average number of pets the drone lost track of within two hours is 3.17 times, and the average recovery rate after losing track is 53.7%. The drone has a better real-time tracking effect, as shown in Figure 12.



Figure 12: Actual identification renderings

6. Summary and Future Anticipations

The STM32-powered drone driver is equipped with an impressive set of features that make it a versatile and useful tool for pet owners. It possesses the ability to follow pets and clean up their waste. Additionally, the drone benefits from a highly advanced stabilization algorithm, enabled by PID algorithm, which ensures smooth and precise flight control even in challenging conditions. Although this drone is currently only a prototype, it has the potential to inspire further innovation and improvement in the field of drone technology, paving the way for more advanced features and capabilities to be incorporated on future iterations.

References

- [1] Anita Domańska, Orzechowski A, Litwiniuk A, et al. *The Beneficial Role of Natural Endocrine Disruptors: Phytoestrogens in Alzheimer's Disease*[J]. *Oxidative Medicine and Cellular Longevity*, 2021, 2021(2). DOI:10.1155/2021/3961445.
- [2] Kumar G, Prasad R, Mahajan P, et al. *Tracking the Progression & Influence of Beta-Amyloid Plaques Using Percolation Centrality and Collective Influence Algorithm: A Study using PET images* [J]. *Cold Spring Harbor Laboratory Press*, 2021. DOI:10.21203/RS.3.RS-277919/V1.
- [3] *Pet Tracking Systems Market to Witness Huge Growth by 2025: Key Players - Marco Polo, POD, Link AKC, Tractive, Whistle* [J]. *M2 Presswire*, 2018.
- [4] *Pet Tracking Systems Market: Comprehensive Study Explores Huge Growth In Future | Tractive, Whistle, Roam EO, The Locator, Tractive* [J]. *M2 Presswire*, 2018
- [5] Manwell S ,Klein R ,Xu T , et al. *Data-driven respiratory gating in cardiac PET/CT using the Positron Emission Tracking algorithm*[J]. *The Journal of Nuclear Medicine*, 2018,59
- [6] Artem M, Jean L, Shin Y D, et al. *A novel two-stage iterative vessel tracking algorithm for determining an image derived input function for PET*[J]. *Journal Of Nuclear Medicine*, 2016, 57